



HAL
open science

Liquid-vapor coexistence in square-well fluids: a RHNC study

Achille Giacometti, Giorgio Pastore, Fred Lado

► **To cite this version:**

Achille Giacometti, Giorgio Pastore, Fred Lado. Liquid-vapor coexistence in square-well fluids: a RHNC study. *Molecular Physics*, 2009, 107 (04-06), pp.555-562. 10.1080/00268970902889642. hal-00513284

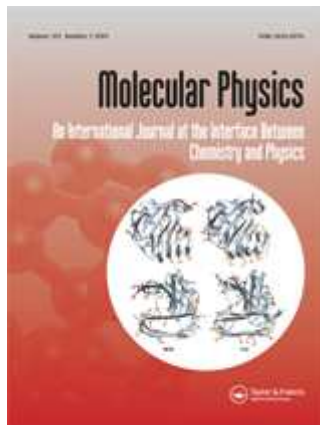
HAL Id: hal-00513284

<https://hal.science/hal-00513284>

Submitted on 1 Sep 2010

HAL is a multi-disciplinary open access archive for the deposit and dissemination of scientific research documents, whether they are published or not. The documents may come from teaching and research institutions in France or abroad, or from public or private research centers.

L'archive ouverte pluridisciplinaire **HAL**, est destinée au dépôt et à la diffusion de documents scientifiques de niveau recherche, publiés ou non, émanant des établissements d'enseignement et de recherche français ou étrangers, des laboratoires publics ou privés.



Liquid-vapor coexistence in square-well fluids: a RHNC study

Journal:	<i>Molecular Physics</i>
Manuscript ID:	TMPH-2008-0444.R1
Manuscript Type:	Special Issue Paper - Dr. Jean-Jacques Weis
Date Submitted by the Author:	09-Mar-2009
Complete List of Authors:	Giacometti, Achille; Università Ca' Foscari, Chimica Fisica Pastore, Giorgio; Università di Trieste, Theoretical Physics Lado, Fred; North Carolina State University, Physics
Keywords:	Theory of liquids, Phase diagrams, Liquid-vapor coexistence, Integral equations, Square-Well fluid
<p>Note: The following files were submitted by the author for peer review, but cannot be converted to PDF. You must view these files (e.g. movies) online.</p> <p>SWrevised2.tex</p>	



Liquid-vapor coexistence in square-well fluids: an RHNC study

Achille Giacometti^a, Giorgio Pastore^{b*}, and Fred Lado^c

9th March 2009

Abstract

We investigate the ability of the reference hypernetted-chain integral equation to describe the phase diagram of square-well fluids with four different ranges of attraction. Comparison of our results with simulation data shows that the theory is able to reproduce with fairly good accuracy a significant part of the coexistence curve, provided an extrapolation procedure is used to circumvent the well-known pathologies of the pseudo-spinodal line, which are more severe at reduced width of the attractive well. The method provides a useful approach for a quick assessment of the location of the liquid-vapor coexistence curve in this kind of fluid and serves as a check for the more complex problem of anisotropic “patchy” square-well molecules.

Pacs numbers: 64.70.F-, 61.20.Gy, 64.60.Ej, 65.20.Jk

Keywords: Theory of liquids, Phase diagrams, Liquid-vapor coexistence, Integral equations, Square-Well fluid.

1
2
3
4 ^aDipartimento di Chimica Fisica, Università Ca' Foscari, S. Marta DD 2137,
5
6 I-30123 Venezia, Italy

7
8 ^bDipartimento di Fisica Teorica dell' Università, Strada Costiera 11, 34014
9
10 Trieste, Italy

11
12 ^cPhysics Department, North Carolina State University, Raleigh, North Car-
13
14 olina 27695-8202

15
16 *Corresponding author. Email: pastore@ts.infn.it
17
18
19
20
21
22
23
24
25
26
27
28
29
30
31
32
33
34
35
36
37
38
39
40
41
42
43
44
45
46
47
48
49
50
51
52
53
54
55
56
57
58
59
60

Introduction

Structural and thermodynamic properties of the square-well (SW) fluid have been studied with a huge variety of statistical mechanical methods. This system has long been viewed as the simplest nontrivial model able to capture the main phenomenology of real atomic fluids by complementing hard-sphere repulsion with a finite-range and constant attractive well [1]. Almost all theories for the liquid state have been applied to the study of the SW fluid and many numerical simulation studies have been published [2, 3, 4, 5, 6, 7, 8, 9, 10, 11, 12, 13, 14], transforming this system into an important testbed for theories [2, 15, 16, 17, 18, 19, 20].

More recently, the study of colloids and protein solutions has renewed interest in SW fluids as a tool to study trends and general features of strongly localized isotropic attractions. However, more detailed investigations of such systems suggest that the isotropic model should be modified to account for highly directional (patchy) interactions [21]. The recent model studied by Kern and Frenkel [22] can be described as a SW model where the potential well has finite *angular* extent as well as finite *radial* extent.

A key problem with such patchy fluids is the determination of their phase diagram. Specialized computer simulation methods have been developed to allow efficient and reliable determination of liquid-vapor coexistence. While applications to atomic systems is nowadays an almost trivial exercise, numerical simulation in the presence of highly attractive and directional forces is still a challenging and time-consuming task. Theoretical modeling, albeit approximate, may provide a worthwhile tool for faster and wide-ranging scans

1
2
3
4 of the relevant parameter space. For such purposes, perturbation methods
5
6 have been used extensively in the past, but their accuracy in the presence of
7
8 strongly directional attractions is not uniform. Alternatively, modern inte-
9
10 gral equation theories are known to provide reliable and accurate description
11
12 of structural properties for isotropic [17, 23] as well as anisotropic poten-
13
14 tials [24]. It is true that in the vicinity of a liquid-vapor critical point they
15
16 manifest shortcomings ranging from branching of multiple unphysical solu-
17
18 tions [25] to wrong critical behavior [17]. Notwithstanding such limitations,
19
20 we believe that integral equation approach is still able to provide a quick
21
22 and reasonably reliable description of the phase diagram. Although results
23
24 for fluid-fluid coexistence from modern integral equation theories are rela-
25
26 tively scarce, the existing evidence shows that they may provide an accurate
27
28 description of the low temperature part of the binodal curve and, by ex-
29
30 trapolation, make it possible to approximately locate the critical point in
31
32 one-component [17, 26] and two-component systems [27]. More accurate ap-
33
34 proximations, such as SCOZA or HRT, have been applied to the SW fluid
35
36 [19, 20], but their implementation for anisotropic interactions is not an easy
37
38 task.
39

40
41 Motivated by an interest in applying the reference hypernetted chain
42
43 (RHNC) approximation [23] to simple *anisotropic* models of patchy colloids,
44
45 as a preliminary step we wanted to understand the limits and shortcomings
46
47 of the integral equation approach to such systems. For this reason, we have
48
49 undertaken here the study of the liquid-vapor coexistence of an *isotropic* SW
50
51 fluid, the extreme limit of patchy SW potentials, using the RHNC approxi-
52
53 mation.
54

1
2
3
4 The RHNC approximation has been used before to study SW fluids [16]
5
6 but, so far as we know, it has not been used to study phase coexistence in
7
8 such systems nor it has been tested at temperatures below the critical tem-
9
10 perature. In this communication, we report results for structural properties
11
12 and liquid-vapor coexistence of a few SW fluids of varying attraction range.
13
14 The plan of the paper is the following: In section 2, we summarize the basic
15
16 RHNC theory and discuss the computational details of our calculation of the
17
18 phase coexistence curve. Results are presented and critically discussed in
19
20 section 3. A short summary of our findings and conclusions is assembled in
21
22 the final section.
23
24
25
26

27 **1 RHNC theory and phase coexistence cal-** 28 29 30 **culations** 31 32

33 We consider a system of spherical particles of diameter σ interacting via a
34
35 pair-wise square-well potential $\phi(r)$ given by
36
37

$$38 \phi(r) = \begin{cases} 39 \infty, & r < \sigma \\ 40 -\epsilon, & \sigma \leq r \leq \lambda\sigma, \\ 41 0, & \lambda\sigma < r \end{cases}$$

42
43
44
45

46 where ϵ is the depth and λ the dimensionless extent of the potential well.
47
48 Reduced temperature and density are introduced as usual using ϵ and σ as
49
50 energy and length scale respectively: $T^* = k_B T / \epsilon$, $\rho^* = \rho \sigma^3$.
51
52
53
54
55

1.1 RHNC integral equation

The pair distribution function $g(r)$ of a classical fluid is related to the pair potential $\phi(r)$ by the exact relation [28]

$$g(r) = \exp[-\beta\phi(r) + h(r) - c(r) + B(r)], \quad (1)$$

where $\beta = 1/k_B T$ is the inverse Kelvin temperature, $h(r) = g(r) - 1$ is the pair correlation function, and $c(r)$ is the direct correlation function defined via the Ornstein-Zernike (OZ) equation,

$$h(r) = c(r) + \rho \int d\mathbf{r}' c(|\mathbf{r} - \mathbf{r}'|) h(r'). \quad (2)$$

It is more convenient for numerical work to solve equations (1) and (2) for the indirect correlation function $\gamma(r) = h(r) - c(r)$ with the OZ equation de-convoluted in Fourier space; the pair of equations to solve then becomes

$$c(r) = \exp[-\beta\phi(r) + \gamma(r) + B(r)] - 1 - \gamma(r), \quad (3)$$

$$\tilde{\gamma}(k) = \frac{\rho \tilde{c}^2(k)}{1 - \rho \tilde{c}(k)}. \quad (4)$$

These equations are connected through the transforms

$$\tilde{c}(k) = \frac{4\pi}{k} \int_0^\infty dr r c(r) \sin(kr) \quad (5)$$

following equation (3) and

$$\gamma(r) = \frac{1}{2\pi^2 r} \int_0^\infty dk k \tilde{\gamma}(k) \sin(kr) \quad (6)$$

following equation (4) to form an iteration cycle. The so-called bridge function $B(r)$ that appears above is a complicated functional of the pair correlation function for which no exact computable expression is known. The various integral equation formulations found in the literature correspond to different approximate forms for $B(r)$.

The SW direct correlation function $c(r)$ is of course discontinuous at $r = \sigma$ and $r = \lambda\sigma$. To compute its Fourier transform (5), we assign the single value of $c(r)$ at a discontinuity to be the arithmetic mean of its separate values at the discontinuity [29]; e.g.,

$$c(\lambda\sigma) = \lim_{\varepsilon \rightarrow 0} \frac{c(\lambda\sigma + \varepsilon) + c(\lambda\sigma - \varepsilon)}{2}. \quad (7)$$

We further ensure that the discontinuities fall on calculated grid points in r . Moreover, note that it is only the short-ranged direct correlation function $c(r)$ that is expected to vanish at large r ; i.e., its Fourier transform requires $c(r_{\max}) = 0$, where r_{\max} is the cutoff distance in the r grid. In the discrete notation used below, $r_{\max} = N_r \Delta r$. The pair correlation function $h(r)$, on the other hand, may have whatever long-range tail it wishes without affecting the calculation.

The RHNC closure [23] assumes that the unknown bridge function $B(r)$ can be approximated by the corresponding known bridge function $B_0(r)$ of a

reference system. Within this approach, just as in the original hypernetted-chain closure [30], the excess Helmholtz free energy per particle can be written in closed form as [23]

$$\frac{\beta A_{\text{ex}}}{N} = \frac{\beta A_1}{N} + \frac{\beta A_2}{N} + \frac{\beta A_3}{N}, \quad (8)$$

where

$$\frac{\beta A_1}{N} = -\frac{1}{2}\rho \int d\mathbf{r} \left\{ \frac{1}{2}h^2(r) + h(r) - g(r) \ln [g(r)e^{\beta\phi(r)}] \right\}, \quad (9)$$

$$\frac{\beta A_2}{N} = -\frac{1}{2\rho} \int \frac{d\mathbf{k}}{(2\pi)^3} \left\{ \ln [1 + \rho\tilde{h}(k)] - \rho\tilde{h}(k) \right\}, \quad (10)$$

$$\frac{\beta A_3}{N} = \frac{\beta A_3^0}{N} - \frac{1}{2}\rho \int d\mathbf{r} [g(r) - g_0(r)] B_0(r). \quad (11)$$

Equation (11) directly expresses the RHNC approximation; here A_3^0 is the corresponding reference system contribution, computed from the known free energy A^0 of the reference system as $A_3^0 = A^0 - A_1^0 - A_2^0$, with A_1^0 and A_2^0 calculated as above but with reference system quantities.

Length and energy parameters of the reference system, respectively σ_0 and ϵ_0 , should be optimized by variational minimization to obtain the free energy from equation (8), which leads [31] to the conditions (written here in dimensionless forms)

$$\rho \int d\mathbf{r} [g(r) - g_0(r)] \sigma_0 \frac{\partial B_0(r)}{\partial \sigma_0} = 0, \quad (12)$$

$$\rho \int d\mathbf{r} [g(r) - g_0(r)] \epsilon_0 \frac{\partial B_0(r)}{\partial \epsilon_0} = 0. \quad (13)$$

These guarantee thermodynamic consistency between the direct calculations

of the pressure P and internal energy U using $g(r)$,

$$\beta P = \rho - \frac{1}{6} \rho^2 \int \mathrm{d}\mathbf{r} g(r) r \frac{d\beta\phi(r)}{dr}, \quad (14)$$

$$\frac{U}{N} = \frac{1}{2} \rho \int \mathrm{d}\mathbf{r} g(r) \phi(r), \quad (15)$$

and the corresponding thermodynamic derivatives of the free energy, $\beta P - \rho = \rho^2 \partial(\beta A_{\text{ex}}/N)/\partial\rho$ and $U/N = \partial(\beta A_{\text{ex}}/N)/\partial\beta$. At present, however, only the hard sphere (HS) system, with sphere diameter σ_0 but no energy scale, is well enough known to serve as reference system. With this choice, only equation (12) is implemented here for the results of the next section.

We will thus obtain the two main ingredients needed, pressure and chemical potential, in a consistent way with no additional approximations beyond the choice of hard spheres as reference system. Any inaccuracy in the computed results can be ascribed solely to the quality of the chosen bridge function.

We solve the RHNC equations numerically on r and k grids of $N_r = 2048$ points with intervals $\Delta r = 0.01\sigma$ and $\Delta k = \pi/(N_r \Delta r)$ using the combination of Newton-Raphson and Picard methods introduced by Gillan [32] and optimized by Labík et al. [33]. Fourier transforms are evaluated with the Fast Fourier Transform algorithm. Sample calculations with the same $\Delta r = 0.01\sigma$ but increased $N_r = 4096$ and $N_r = 8192$ produce *identical* results for all the printed output; i.e., to four or five significant figures.

For the bridge function, we use the Verlet-Weis-Henderson-Grundke (VWHG) parametrization of HS numerical simulation results [34, 35]. The HS free energy is taken from the Carnahan-Starling equation of state [36],

which is also incorporated into the VWHG parametrization. Other parametrizations exist and in the only previous investigation of the SW fluid with RHNC, at supercritical temperatures, Gil-Villegas et al. [16] used that of Malijevský and Labík [37, 38] and found excellent agreement with computer simulation results for thermodynamics and correlation functions. In the present study we choose VWHG bridge functions because they have been frequently used in RHNC calculations (also for liquid-vapor coexistence of HS Yukawa [39] fluids), thus allowing a direct comparison of the performances of the approximation with different potentials.

1.2 Liquid-vapor coexistence

Two-phase coexistence at constant temperature requires the equality of pressure and chemical potential of the two phases; RHNC provides convenient expressions for both quantities,

$$\beta P = \rho + \frac{2}{3} \pi \rho^2 \sigma^3 \left[y(\sigma) e^{\beta \epsilon} - \lambda^3 y(\lambda \sigma) (e^{\beta \epsilon} - 1) \right], \quad (16)$$

$$\beta \mu = \frac{\beta A_{\text{ex}}}{N} + \left(\frac{\beta P}{\rho} - 1 \right) + \ln(\rho \sigma^3), \quad (17)$$

where we have now specialized the pressure equation (14) for the SW potential and we are using the cavity function $y(r) = g(r) \exp[\beta \phi(r)]$, which has no discontinuities. An additional density-independent term from the ideal gas limit has been neglected in the total chemical potential μ .

In order to find the densities of the two coexisting phases, we use the following procedure [41]: we start two calculations, one at low density and

the other at high density at the temperature of interest. Then, density is increased from the lowest value and decreased from the highest until either the coexistence conditions are satisfied or the numerical program is unable to converge, **even after systematic reduction of the density change**, signaling the disappearance of a solution of the integral equation. Conditions of equal pressure and chemical potential are verified by looking for numerical solutions of the nonlinear set of equations,

$$\beta P(\rho_l) = \beta P(\rho_g), \quad (18)$$

$$\beta \mu(\rho_l) = \beta \mu(\rho_g), \quad (19)$$

where ρ_g and ρ_l denote respectively the density of the gas and of the liquid. The possibility of coexistence can be visually checked by plotting in a $(\beta P, \beta \mu)$ plane the high and the low density branches. A crossing of the two curves signals the occurrence of phase coexistence. The exact determination of the intersection point is performed numerically by using cubic spline interpolations through the calculated points.

Ideally, one should get crossings along the whole binodal line, from lowest accessible temperature up to the critical point. In practice, the approximate nature of RHNC, shared with all integral equations, introduces thermodynamic inconsistencies and modifies the singular behavior of the spinodal line obtained from the fluctuation route. It is transformed into a pseudo-spinodal line of branching points where the real solution of the equations does not show a divergence of the structure factor $S(0) = 1 + \rho \tilde{h}(0)$ at zero wavenumber or, equivalently, a vanishing of the inverse long-wavelength (lw) isothermal

compressibility

$$\beta \left. \frac{\partial P}{\partial \rho} \right|_{lw} = 1 - \rho \tilde{c}(0). \quad (20)$$

Moreover, such a pseudo-spinodal line extends the no-solution region into a non-negligible neighborhood of the critical point, thus preempting the possibility of finding the coexisting densities. As a result, the possibility of getting the coexistence curve with integral equations is limited to relatively low temperatures. In a way, the quality of an integral equation can be accurately tested by the extent of the resulting coexistence curve.

In the case of SW fluids we have found, as discussed in the next section, that reducing the width of the SW progressively extends the temperature interval below the critical point where the pseudo-spinodal line preempts the binodal. However, we note that the quality of the thermodynamic and structural data in the accessible region of the phase diagram remains high. Thus, we have investigated the possibility of a small extrapolation of the RHNC data inside the pseudo-spinodal region. In all the cases we have investigated, such extrapolation is required only in the gas phase and the resulting coexistence curve appears as a smooth continuation of the part based on real crossings.

In figure 1, we show a typical case of quasi-crossing while figure 2 shows a case of a more distant missed crossing. In both cases, the possibility of finding a coexisting vapor phase is preempted by the sudden disappearance of the low-density solution. It is clear that, although RHNC does not have a low-density solution at the same temperature and pressure of a corresponding liquid, a smooth extrapolation of thermodynamic data could be quite safe in

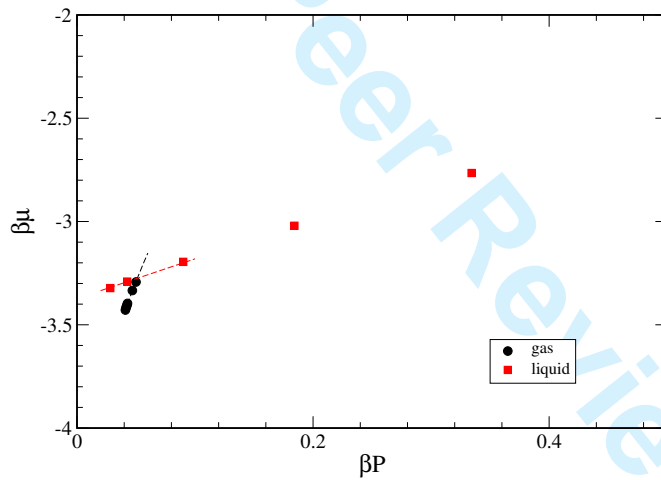


Figure 1: Determination of the coexistence point. Case of quasi-crossing at $T^* = 2.5$, $\lambda = 2$. Squares: liquid branch; circles: vapor branch. Dashed lines indicate the cubic spline approximation used to locate the extrapolated crossing point.

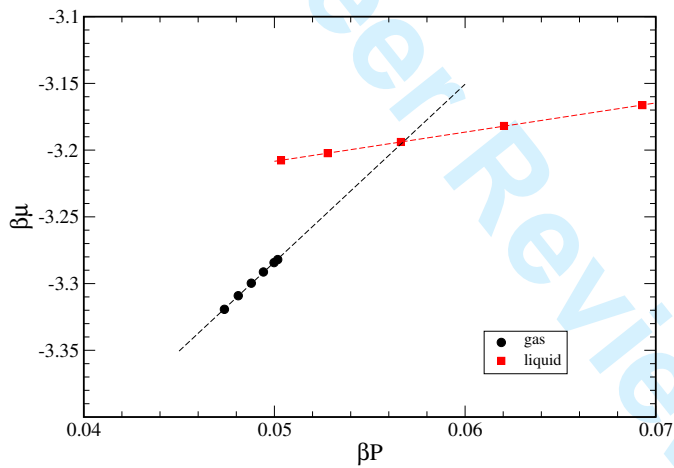


Figure 2: Determination of the coexistence point. Case of a large extrapolation at $T^* = 1.74$, $\lambda = 1.75$. Symbols as in figure 1.

cases like that in figure 1, due to the small curvature of the lines and to their strong transversality. Larger extrapolations, like that in figure 4, appear to introduce uncontrolled uncertainties. Additional comments will be added in the next section.

2 Results

As a first check of the RHNC quality, we have computed the pressure P and excess chemical potential

$$\beta\mu_{\text{ex}} = \frac{\beta A_{\text{ex}}}{N} + \left(\frac{\beta P}{\rho} - 1 \right) \quad (21)$$

for states at high densities with $\lambda = 1.5$ examined by Labík et al. [40] using scaled-particle Monte Carlo (SP-MC) simulation at $\rho^* = 0.8$ and 0.9 . Results for the pressure from simulation and the RHNC calculation are compared in figure 3, while figure 4 gives the comparisons for the excess chemical potential. There is overall quite good agreement, although the weakening of the RHNC results with increasing density and decreasing temperature, a shortcoming common to all integral equation closures, does become evident.

In tables 1 and 2 we report a few significant comparisons between RHNC thermodynamic and structural results and recent numerical simulation data [42, 8] for SW systems of different range.

We notice a progressive worsening of thermodynamic results for stronger couplings, meaning lower temperatures and higher densities, and for decreasing λ . Such behavior as a function of well width is understandable, since in

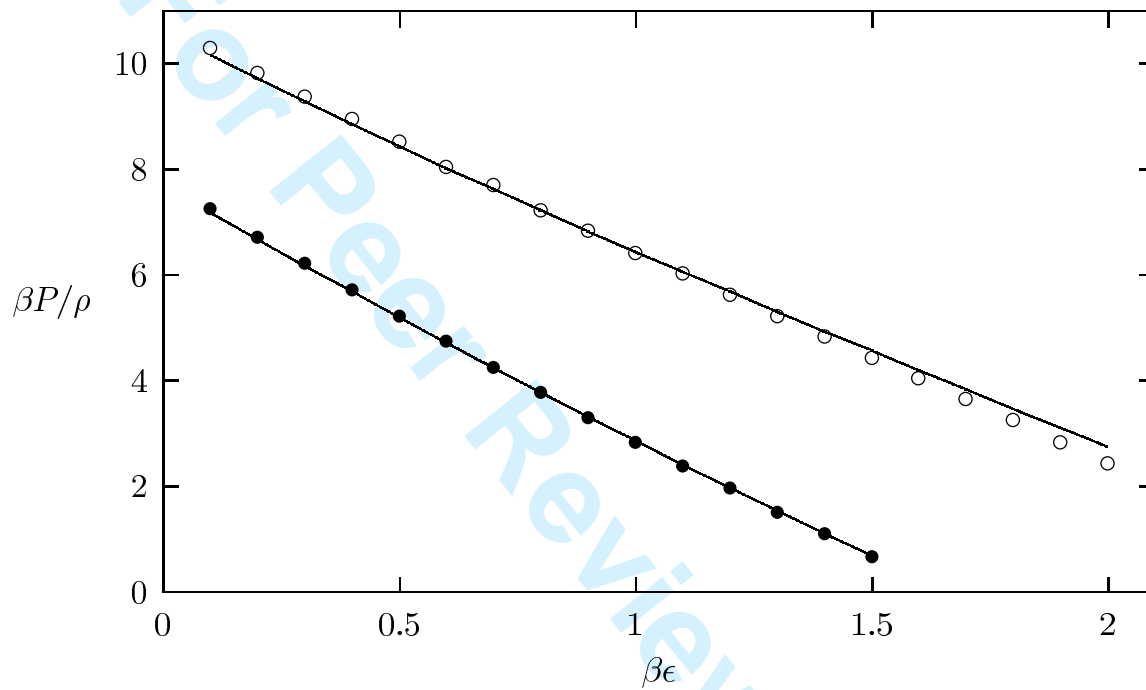


Figure 3: SP-MC pressure vs. inverse temperature for a SW fluid with $\lambda = 1.5$ obtained by Labík et al. [40] at $\rho^* = 0.8$ (filled circles) and $\rho^* = 0.9$ (empty circles). Solid lines are the RHNC results.

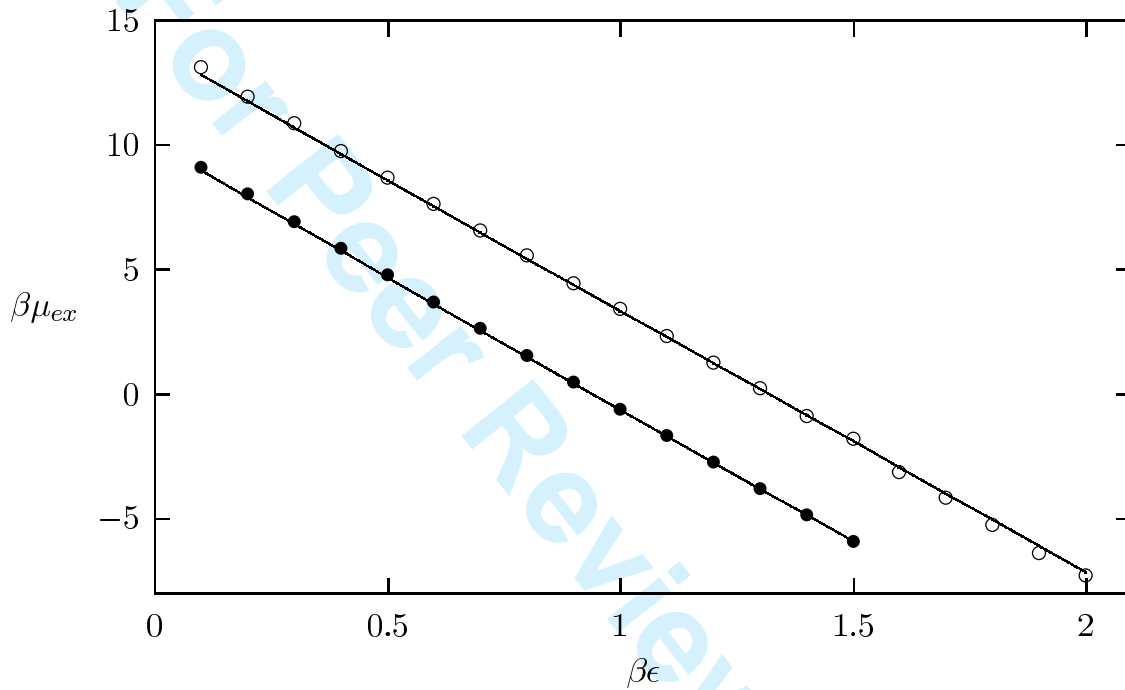


Figure 4: SP-MC chemical potential vs. inverse temperature for a SW fluid with $\lambda = 1.5$ obtained by Labík et al. [40] at $\rho^* = 0.8$ (filled circles) and $\rho^* = 0.9$ (empty circles). Solid lines are the RHNC results.

Table 1: Comparison of simulation and RHNC thermodynamic quantities of square-well fluids. For each density, the first row contains Monte Carlo data of Largo and Solana [42] and the second row our results.

		$\beta P/\rho$	$-U/N\epsilon$	$\beta P/\rho$	$-U/N\epsilon$	$\beta P/\rho$	$-U/N\epsilon$
$\lambda = 1.2$	ρ^*	$T^* = 0.7$		$T^* = 1.0$		$T^* = 3.0$	
	0.1	0.76	0.62	0.96	0.40	1.17	0.23
		0.76	0.62	0.96	0.40	1.17	0.23
	0.8	0.77	3.68	2.72	3.43	6.03	3.09
		0.68	3.58	2.68	3.38	5.99	3.09
$\lambda = 1.5$		$T^* = 1.5$		$T^* = 3.0$			
	0.1	0.78	0.92	1.03	0.69		
		0.78	0.92	1.03	0.69		
	0.7	2.31	5.28	4.02	5.08		
		2.30	5.27	3.98	5.07		
$\lambda = 2.0$		$T^* = 3.0$		$T^* = 5.0$			
	0.1	0.69	1.96	0.91	1.72		
		0.69	1.98	0.92	1.73		
	0.6	1.19	9.75	2.44	9.58		
		1.18	9.76	2.43	9.59		
	0.7	2.01	11.35	3.51	11.16		
		1.97	11.35	3.47	11.16		

Table 2: Comparison of simulation and RHNC contact values $g(\sigma^+)$, $g(\lambda\sigma^-)$ and $g(\lambda\sigma^+)$ of the radial distribution function of square-well fluids. Monte Carlo data (MC) from Largo et al. [8].

λ	T^*	ρ^*	$g(\sigma^+)$		$g(\lambda\sigma^-)$		$g(\lambda\sigma^+)$	
			MC	RHNC	MC	RHNC	MC	RHNC
1.1	0.5	0.1	7.254	7.260	7.179	7.179	0.966	0.973
		0.5	6.088	5.835	5.816	5.460	0.787	0.739
		0.7	5.667	5.681	5.307	4.967	0.718	0.672
1.2	0.7	0.1	4.126	4.150	4.030	4.046	0.968	0.970
		0.5	3.449	3.272	3.122	2.945	0.748	0.706
		0.7	3.281	3.186	2.810	2.744	0.675	0.658
1.5	1.5	0.1	1.952	1.957	1.832	1.835	0.941	0.944
		0.5	1.989	1.994	1.382	1.382	0.709	0.709
		0.7	2.783	2.770	1.115	1.149	0.590	0.590
	2.0	0.1	1.661	1.655	1.563	1.561	0.945	0.947
		0.5	2.006	2.003	1.274	1.272	0.771	0.772
		0.7	2.880	2.865	1.063	1.061	0.646	0.644
1.8	2.0	0.1	1.839	1.914	1.599	1.642	0.974	0.996
		0.5	2.199	2.211	1.175	1.181	0.714	0.716
		0.7	3.487	3.474	1.141	1.147	0.693	0.695
	3.0	0.1	1.449	1.456	1.320	1.320	0.942	0.945
		0.5	2.162	2.162	1.079	1.080	0.773	0.774
		0.7	3.392	3.365	1.043	1.045	0.747	0.751

1
2
3
4 the limit of very large λ and vanishing ϵ , the properties of SW fluid should
5
6 be well described by HS physics, supplemented by the van der Waals mean
7
8 field approximation. In such a limit RHNC should provide very accurate
9
10 results. In the opposite case, we would expect the maximum deviation from
11
12 the hypothesis of universality of the bridge function and then the maximum
13
14 discrepancy from simulation. In the only previous RHNC study of SW fluid
15
16 that we are aware of, ref. [16], a limited analysis of the differences between
17
18 HS and SW bridge functions has been attempted. In that paper, the authors
19
20 assumed the same functional form for the bridge function outside the hard
21
22 core for both HS and SW systems and determined the parameters via a mean-
23
24 square fitting of Monte Carlo (MC) data via RHNC. Apparently, optimal SW
25
26 bridge functions should be slightly smaller than the best HS functions for the
27
28 same system, but we note that the constrained procedure did not allow for
29
30 qualitative changes of the functional form. We can add that the most im-
31
32 portant for possible changes is the region within and close to the hard core.
33
34 Direct evidence for this comes from a few calculations we performed by mod-
35
36 ifying the long range part of the bridge function in a very crude way: we
37
38 made it vanish starting from its first zero. The resulting RHNC solution was
39
40 almost unaffected by this change, thus confirming that any future effort to
41
42 improve the bridge function beyond the HS approximation should be focused
43
44 on the core interval between zero and the HS diameter.

45
46
47 We have studied the RHNC liquid-vapor coexistence of four SW systems
48
49 of width size $\lambda = 1.25, 1.5, 1.75,$ and 2 . In figures 5-8 we present our
50
51 results for the coexistence curves of the four SW fluids we have examined.
52
53 RHNC data (squares connected by a line) are compared with different sets
54
55

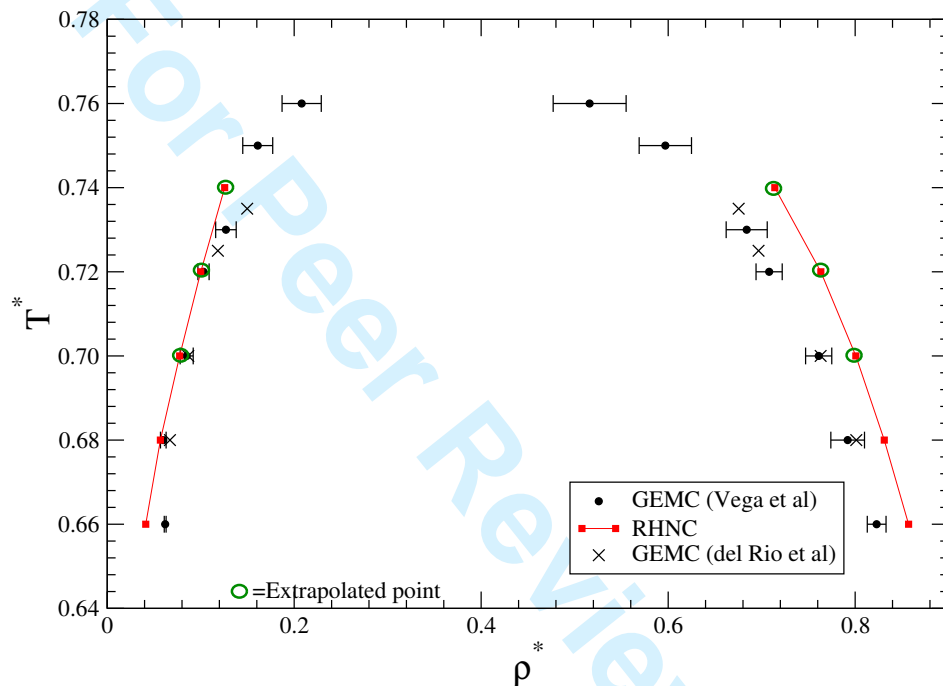


Figure 5: Vapor-liquid T^* versus ρ^* coexistence for the SW fluid of range $\lambda = 1.25$: squares, this work (circled squares indicate extrapolation of the vapor branch), a line has been drawn through the points as a visual guide; dots, Vega et al. [3]; crosses, del Río et al. [5].

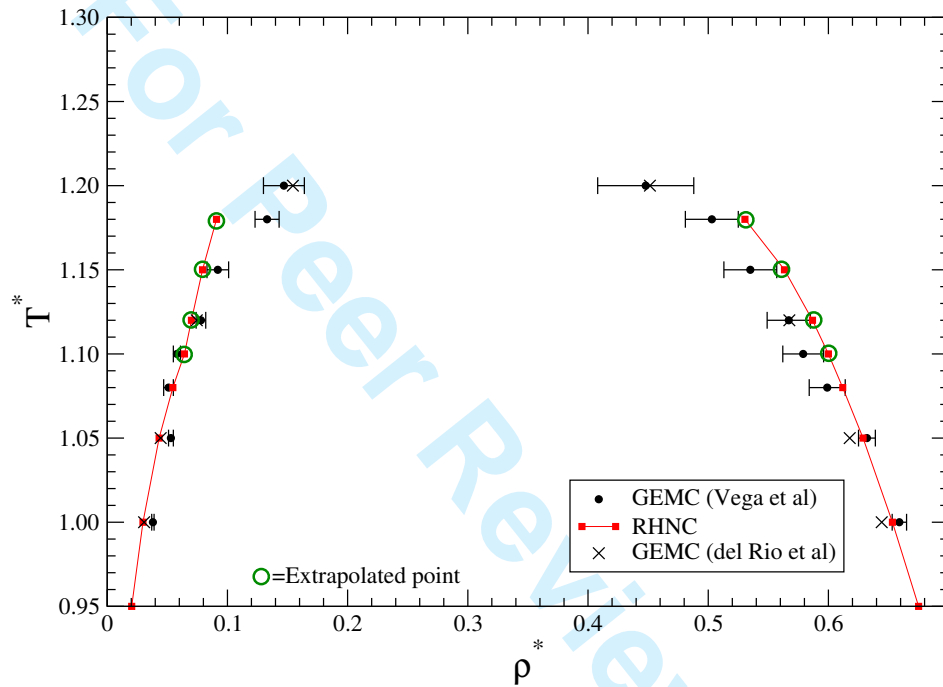


Figure 6: Vapor-liquid T^* versus ρ^* coexistence for the SW fluid of range $\lambda = 1.5$: squares, this work (circled squares indicate extrapolation of the vapor branch), a line has been drawn through the points as a visualguide; dots, Vega et al. [3]; crosses, del R o et al. [5].

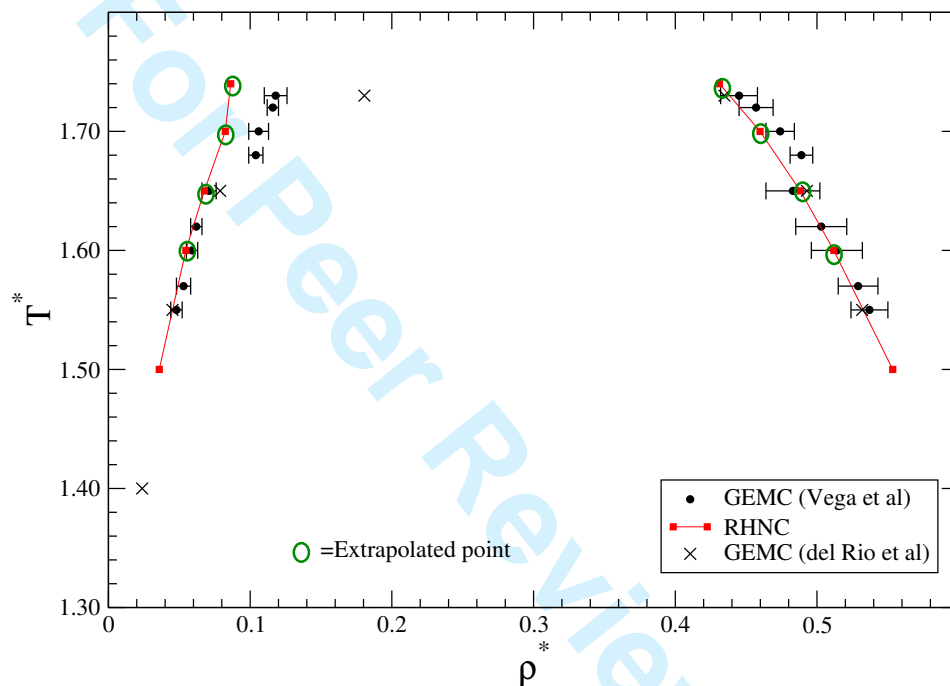


Figure 7: Vapor-liquid T^* versus ρ^* coexistence for the SW fluid of range $\lambda = 1.75$: squares, this work (circled squares indicate extrapolation of the vapor branch), a line has been drawn through the points as a visualguide); dots, Vega et al. [3]; crosses, del Río et al. [5].

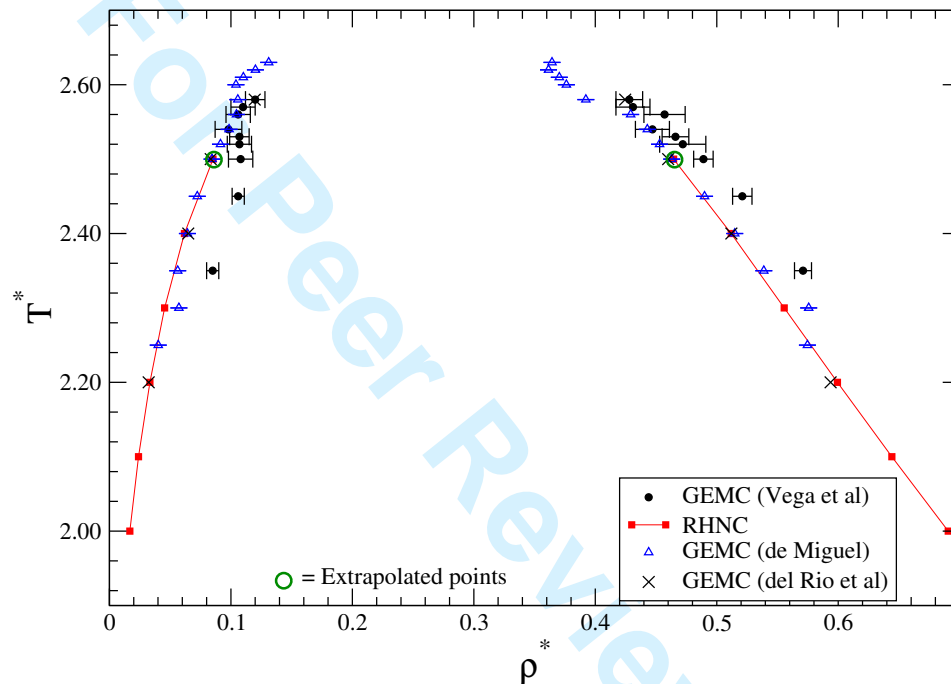


Figure 8: Vapor-liquid T^* versus ρ^* coexistence for the SW fluid of range $\lambda = 2.0$: squares, this work (circled squares indicate extrapolation of the vapor branch), a line has been drawn through the points as a visualguide; dots, Vega et al. [3]; crosses, del R o et al. [5]; triangles, de Miguel [4].

of simulation data (see figure captions). All the cases where RHNC did not provide a real crossing between the two branches (low and high density) of the βP - $\beta\mu$ curves have been marked by a circle around the square.

Two main features of the results are evident: the overall semiquantitative accuracy of the coexistence curve in all the investigated cases and the progressive worsening of the quality of the RHNC results as the range λ is reduced. The latter appears as the obvious consequence, at the level of a phase diagram, of our observations about the quality of thermodynamic data as a function of the range. At $\lambda = 2$, our results closely follow the data of de Miguel [4] and of del Río et al. [5], while Gibbs ensemble Monte Carlo results by Vega et al. [3] seem to be definitely biased toward higher densities. In addition, the unphysical changes of the curvature seen in the MC data suggest that one might consider quite optimistic the published statistical error bars.

At $\lambda = 1.75$, RHNC results start to show clear evidence of a distortion of the coexistence curve at the highest temperature, although all the points below $T^* = 1.70$ are in good agreement with MC data. Since the extrapolation at this temperature corresponds to the case shown in figure 2, while the remaining extrapolations correspond to closer missed intersections, we have a measure of the quantitative effect of our extrapolation procedure on the resulting binodal line.

Data at $\lambda = 1.5$ and $\lambda = 1.25$ clearly show a progressive decrease of the quality on the high density side of the curve. As previously discussed, this region corresponds to the region where RHNC could be substantially affected by improvements in the description of the bridge function. We stress that

1
2
3
4 coexistence is a severe test for the quality of integral equations. In particular,
5
6 pressure and chemical potential are quantities quite sensitive to small changes
7
8 of the closure.
9

10 However, according to Liu et al. [9], at $\lambda = 1.25$ the liquid-vapor transi-
11
12 tion becomes metastable and is preempted by the freezing transition. Thus,
13
14 the observed decreased quality at smaller widths is somewhat compensated
15
16 by the fact that the integral equation results for such case are referring to a
17
18 metastable liquid.
19

20 In all the cases, integral equations do not allow one to get close enough
21
22 to the critical point to provide a direct estimate of its location. However,
23
24 a good quality in reproducing the low temperature part of the liquid vapor
25
26 coexistence and the hypothesis of Ising-like value for the critical exponent
27
28 ($\beta = 0.325$) may provide a first approximation for the extent of the two-
29
30 phase region.
31
32
33
34

35 Conclusions

36
37
38 We have shown that RHNC is able to reproduce the low-temperature part of
39
40 the liquid-vapor phase diagrams of square-well fluids. With increasing tem-
41
42 perature and depending on the extent of the attractive well, there is a region
43
44 of the binodal line that can be obtained by a slight extrapolation of the vapor
45
46 phase beyond the numerical limit of the quasi-spinodal line. Eventually, ap-
47
48 proaching the critical temperature, the extrapolation becomes very poor and
49
50 the shape of the coexistence line is strongly affected. The agreement with
51
52 the best computer simulations is good for the widest well sizes, but becomes
53
54

1
2
3
4 less satisfactory for λ at or below 1.5. Since the only approximation of the
5 theory is the bridge function (apart from inherent limitations of numerical
6 computation), our results point to the need for an improvement of the short
7 range part of the bridge function.
8
9

10
11
12 It is interesting to note also that our results are consistent with similar
13 RHNC calculations on the Lennard-Jones fluid [17, 26], where it is possible
14 to obtain a larger part of the binodal line than in the case of $\lambda = 2$, thus
15 confirming our findings on better performances for wider range potentials.
16
17
18

19
20 We stress again that the main purpose of the present investigation is
21 not to propose RHNC as an alternative to more refined theories such as
22 SCOZA or HRT when a highly accurate description of the critical properties
23 is required. Rather, we have the more limited goal of checking the ability of
24 the RHNC formulation to provide an approximate but quick tool for locating
25 the liquid-vapor phase transition in SW-like systems. In all the isotropic
26 SW cases we have studied, the theory allows one to predict from scratch
27 an unknown phase coexistence in a computational time that is negligible
28 compared to numerical simulations, using existing numerical techniques for
29 integral equation solutions. Such a feature may only be marginally interesting
30 for isotropic SW fluids, but becomes crucial for anisotropic patchy models of
31 globular macromolecules. We are currently investigating this topic.
32
33
34
35
36
37
38
39
40
41
42
43
44

45 After this paper was submitted for publication, a very thorough work
46 on the same topic of liquid-vapor phase equilibrium for the SW fluid us-
47 ing a different integral equation was published by El Mendoub et al. [43].
48 These authors use an efficient “adaptive grid” [44] that automates the map-
49 ping of the no-solution space in the temperature-density plane. Comparing
50
51
52
53
54

1
2
3
4 their results to ours, we notice that RHNC results for the radial distribution
5 function show a uniform better agreement with simulation data. Since de-
6 viations from computer simulation binodal lines shown by their closure and
7 the present study have opposite directions, a detailed comparison between
8 their closure and RHNC would be interesting .
9
10
11
12
13

Acknowledgments

14
15
16 A.G. acknowledges financial support from Miur-Cofin 2008/2009.
17
18
19
20

References

- 21
22
23
24
25 [1] J.A. Barker and D. Henderson, Rev. Mod. Phys. **48**, 587 (1976).
26
27
28 [2] D. Henderson, W.G. Madden, and D.D. Fitts, J. Chem. Phys. **64**, 5026
29 (1976).
30
31
32 [3] L. Vega, E. de Miguel, L.F. Rull, G. Jackson, and I.A. McLure, J. Chem.
33 Phys. **96**, 2296 (1992).
34
35
36 [4] E. de Miguel, Phys. Rev. E **55**, 1347 (1997).
37
38
39 [5] F. del Río, E. Ávalos, R. Espíndola, L.F. Rull, G. Jackson, and S. Lago,
40 Mol. Phys. **100**, 2531 (2002).
41
42
43 [6] Y.C. Kim, M.E. Fisher, and E. Luijten, Phys. Rev. Lett. **91**, 065701
44 (2003).
45
46
47 [7] J.K. Singh, D.A. Kofke, and J.R. Errington, J. Chem. Phys. **119**, 3405
48 (2003).
49
50
51
52
53
54
55
56
57
58
59
60

- 1
2
3
4 [8] J. Largo, J.R. Solana, S.B. Yuste, and A. Santos, *J. Chem. Phys.* **122**,
5 084510 (2005).
6
7
8
9 [9] H. Liu, S. Garde, and S. Kumar, *J. Chem. Phys.* **123**, 174505 (2005).
10
11
12 [10] D.L. Pagan and J.D. Gunton, *J. Chem. Phys.* **122**, 184515 (2005).
13
14 [11] S.B. Kiselev, J.F. Ely, and J.R. Elliott Jr, *Mol. Phys.* **104**, 2545 (2006).
15
16
17 [12] R. López-Rendón, Y. Reyes, and P. Orea, *J. Chem. Phys.* **125** , 084508
18 (2006).
19
20
21
22 [13] R.P. White and J.E.G. Lipson, *Mol. Phys.* **105**, 1983 (2007).
23
24
25 [14] H.L. Vörtler, K. Schäfer, and W.R. Smith, *J. Phys. Chem. B* **112**, 4656
26 (2008).
27
28
29
30 [15] W.R. Smith and D. Henderson, *J. Chem. Phys.* **69**, 319 (1978).
31
32
33 [16] A. Gil-Villegas, C. Vega, F. del Río, and A. Malijevský, *Mol. Phys.* **86**,
34 857 (1995).
35
36
37
38 [17] C. Caccamo, *Phys. Reports* **98**, 1 (1996).
39
40
41 [18] J.A. White, *J. Chem. Phys.* **113**, 1580 (2000).
42
43
44 [19] A. Reiner and G. Kahl, *J. Chem. Phys.* **117**, 4925 (2002).
45
46
47 [20] E. Schöll-Paschinger, A.L. Benavides, and R. Castañeda-Priego, *J.*
48 *Chem. Phys.* **123**, 234513 (2005).
49
50
51 [21] H. Liu, S.K. Kumar, and F. Sciortino, *J. Chem. Phys.* **127**, 084902
52 (2007).
53
54
55

- 1
2
3
4 [22] N. Kern and D. Frenkel, J. Chem. Phys. **118**, 9882 (2003).
5
6
7 [23] F. Lado, S.M. Foiles, and N.W. Ashcroft, Phys. Rev. **A 28**, 2374 (1983).
8
9
10 [24] F. Lado, E. Lomba, and M. Lombardero, J. Chem. Phys. **103**, 481
11 (1995).
12
13 [25] L. Belloni, J. Chem. Phys. **98**, 8080 (1993).
14
15 [26] E. Lomba, Mol. Phys. **68**, 87 (1989).
16
17 [27] G. Pastore, R. Santin, S. Taraphder, and F. Colonna, J. Chem. Phys.
18 **122**, 181104 (2005).
19
20 [28] J.P. Hansen and I.R. McDonald, *Theory of Simple Liquids* (Academic,
21 New York, 1986).
22
23 [29] See, for example, G. Arfken, *Mathematical Methods for Physicists* (Aca-
24 demic, Orlando, 1985), p. 763.
25
26 [30] T. Morita and K. Hiroike, Prog. Theor. Phys. **23**, 1003 (1960).
27
28 [31] F. Lado, Phys. Lett. **89A**, 196 (1982).
29
30 [32] M. Gillan, Mol. Phys. **38**, 1782 (1979).
31
32 [33] S. Labík, A. Malijevský, and P. Voňka, Mol. Phys. **56**, 709 (1985).
33
34 [34] L. Verlet and J-J. Weis, Phys. Rev. A **5**, 939 (1972).
35
36 [35] D. Henderson and E.W. Grundke, J. Chem. Phys. **63**, 601 (1975).
37
38 [36] N.F. Carnahan and K.E. Starling, J. Chem. Phys. **51**, 635 (1969).
39
40
41
42
43
44
45
46
47
48
49
50
51
52
53
54
55

60

- 1
2
3
4 [37] A. Malijevský and S. Labík, Mol. Phys. **60**, 663 (1987).
5
6
7 [38] S. Labík and A. Malijevský, Mol. Phys. **67**, 431 (1989).
8
9
10 [39] E. Lomba and N.G. Almarza, J. Chem. Phys. **100**, 8367 (1994).
11
12
13 [40] S. Labík, A. Malijevský, R. Kao, W.R. Smith, and F. del Río, Mol.
14 Phys. **96**, 849 (1999).
15
16
17 [41] A.G. Schlijper, H.M. Telo da Gama, and P.G. Ferreira, J. Chem. Phys.
18 **98**, 1534 (1993).
19
20
21
22 [42] J. Largo and J.R. Solana, Phys. Rev. E **67**, 066112 (2003), EDAPS Doc-
23 ument No. EPAPS E-PLLEE8-67-132306 ,reachable from the EPAPS
24 home page (<http://www.aip.org/pubservs/epaps.html>)
25
26
27
28
29 [43] E.B. El Mendoub, J.-F. Wax, I. Charpentier, and N. Jakse, Mol. Phys.
30 **106**, 2667 (2008).
31
32
33
34 [44] I. Charpentier and N. Jakse, J. Chem. Phys. **123**, 204910 (2005).
35
36
37
38
39
40
41
42
43
44
45
46
47
48
49
50
51
52
53
54
55
56
57
58
59
60

Table 1: Comparison of simulated and RHNC thermodynamic quantities of square-well fluids. For each density, the first row contains Monte Carlo data from ref. [42] and the second row our results. The compressibility factor Z is defined as $\beta P/\rho^*$.

$\lambda = 1.2$	ρ^*	$T^* = 0.7$		$T^* = 1.0$		$T^* = 3.0$	
		Z	$-U/N\epsilon$	Z	$-U/N\epsilon$	Z	$-U/N\epsilon$
0.1		0.76	0.62	0.96	0.40	1.17	0.23
		0.76	0.62	0.96	0.40	1.17	0.23
0.8		0.77	3.68	2.72	3.43	6.03	3.09
		0.68	3.58	2.68	3.38	5.99	3.09
$\lambda = 1.5$	0.1	$T^* = 1.5$		$T^* = 3.0$			
		0.78	0.92	1.03	0.69		
0.7		0.78	0.92	1.03	0.69		
		2.31	5.28	4.02	5.08		
0.6		2.30	5.27	3.98	5.07		
$\lambda = 2.0$	0.1	$T^* = 3.0$		$T^* = 5.0$			
		0.69	1.96	0.91	1.72		
0.6		0.69	1.98	0.92	1.73		
		1.19	9.75	2.44	9.58		
0.7		1.18	9.76	2.43	9.59		
		2.01	11.35	3.51	11.16		
		1.97	11.35	3.47	11.16		

Table 1: Comparison of simulation and RHNC contact values $g(\sigma^+)$, $g(\lambda\sigma^-)$ and $g(\lambda\sigma^+)$ of the radial distribution function of square-well fluids. Monte Carlo data (MC) from Largo et al. [8].

λ	T^*	ρ^*	$g(\sigma^+)$		$g(\lambda\sigma^-)$		$g(\lambda\sigma^+)$	
			MC	RHNC	MC	RHNC	MC	RHNC
1.1	0.5	0.1	7.254	7.260	7.179	7.179	0.966	0.973
		0.5	6.088	5.835	5.816	5.460	0.787	0.739
		0.7	5.667	5.681	5.307	4.967	0.718	0.672
1.2	0.7	0.1	4.126	4.150	4.030	4.046	0.968	0.970
		0.5	3.449	3.272	3.122	2.945	0.748	0.706
		0.7	3.281	3.186	2.810	2.744	0.675	0.658
1.5	1.5	0.1	1.952	1.957	1.832	1.835	0.941	0.944
		0.5	1.989	1.994	1.382	1.382	0.709	0.709
		0.7	2.783	2.770	1.115	1.149	0.590	0.590
	2.0	0.1	1.661	1.655	1.563	1.561	0.945	0.947
		0.5	2.006	2.003	1.274	1.272	0.771	0.772
		0.7	2.880	2.865	1.063	1.061	0.646	0.644
1.8	2.0	0.1	1.839	1.914	1.599	1.642	0.974	0.996
		0.5	2.199	2.211	1.175	1.181	0.714	0.716
		0.7	3.487	3.474	1.141	1.147	0.693	0.695
	3.0	0.1	1.449	1.456	1.320	1.320	0.942	0.945
		0.5	2.162	2.162	1.079	1.080	0.773	0.774
		0.7	3.392	3.365	1.043	1.045	0.747	0.751